Off-axis aberration estimation in an EUV microscope using natural speckle

Aamod Shanker[1], Antoine Wojdyla[2], Gautam Gunjala[1], Jonathan Dong[3], Markus Benk[2], Andy Neureuther[1], Kenneth Goldberg[2], Laura Waller[1]

[1] *Dept of Electrical Engineering and Computer Sciences, University of California, Berkeley, CA*
[2] *Center for X-Ray Optics, Lawrence Berkeley National Lab, Berkeley, CA*
[3] *Département de Physique, Ecole Normale Supérieure, Paris 75005, France*
aamodsh@gmail.com

Abstract: Surface roughness on a flat object causes natural speckle when imaged by an extreme ultraviolet (EUV) microscope under sufficient coherence. Using a phase-to-intensity transfer function theory, direct estimation of aberrations from the spectrum of the speckle intensity is demonstrated for various illumination angles.

OCIS codes: 110.4850, 110.6150, 340.7480

1. Phase to intensity transfer function

Extreme ultraviolet (EUV) lithography is under aggressive development for semiconductor manufacturing, because it enables smaller features and thus continued scaling. In the EUV regime, the short wavelength ($\lambda \approx 13.5nm$) means that even very smooth objects cause speckle due to surface roughness at the scale of the wavelength. For reflective surfaces that can be classified as weak phase objects (e.g. EUV lithography masks) a phase-to-intensity transfer function can be defined, which is imaged directly in the speckle spectrum. This transfer function is a function of the system pupil, which is estimated in a subsequent step, characterizing system properties for various illumination angles. Thus, we show that the aberrations in the SHARP EUV microscope [1] can be estimated directly from the weak speckle formed by unavoidable surface roughness.

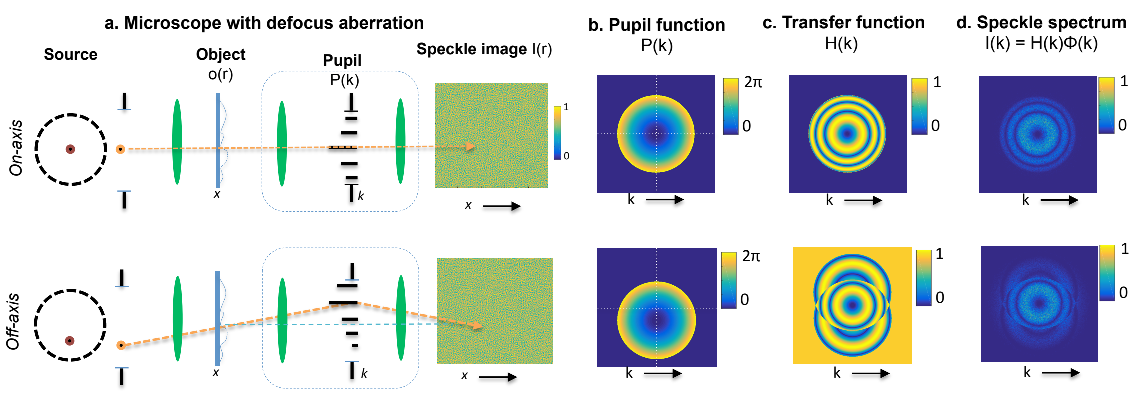

Fig. 1. Phase to intensity transfer function and hence the system pupil can be recovered from the speckle spectrum of a "rough" object in a microscope. a) Schematic of a microscope in on-axis (top) and off-axis (bottom) configurations. b) Pupil of the corresponding transfer function which shifts for off-axis illumination with respect to the object spectrum. c) Phase to intensity transfer function, a combination of pupil and its conjugate, shows two overlapping circles for the off-axis case. d) The spectrum of the speckle reveals the transfer function multiplied by the spectrum of the object phase.

To model a flat surface with some roughness that will cause speckle at the image plane, consider first a thin object that scatters incident light by its absorption ($a(r)$) and phase ($\phi(r)$) over real space r as,

$$o(r) = 1 + a(r)e^{i\phi(r)} = 1 + a(r)cos\phi(r) + ia(r)sin\phi(r) \quad (1)$$

An almost perfectly transparent or reflecting surface ($a(r) \approx constant$) may still have phase due to roughness, which is weak when the phase variation is small ($sin\phi \approx \phi$), hence,

$$o(r) \approx c + i\phi(r) \tag{2}$$

where c is a constant background (assumed to be 1 for further calculation). This is the weak object approximation [2], similar to the Born approximation [3], and holds when the phase variations are approximately limited to some fraction of a wavelength. Image formation for a microscope with a pupil function $P(k)$ (over spatial frequency k) is then obtained by multiplying the spectrum of the object by the pupil, followed by a Fourier transform (Fig. 1a,b top)

$$I(r) = |\mathscr{F}[O(k)P(k)]|^2 \tag{3}$$

where $O(k)$ is the spectrum of $o(r)$, obtained by Fourier transforming Eqn. 2,

$$O(k) = \delta(k) + i\Phi(k) \tag{4}$$

For off-axis illumination, the object spectrum will shift relative to the pupil (Fig. 1a,b bottom), with intensity in Eqn. 3 now given by -

$$I(r) = |\mathscr{F}[O(k-k_l)P(k)]|^2 \tag{5}$$

Next the transfer function that maps the phase of the rough surface to the image intensity, variously referred to as contrast transfer function [2], optical transfer function [4], weak object transfer function [5], coherent transfer function [6] or simply the phase-to-intensity transfer function is derived in the frequency domain. Taking the Fourier transform of Eqn. 5 - absolute value squared becomes autocorrelation in frequency domain [7],

$$I(k) = [O(k-k_l)P(k)] * [O^*(-k-k_l)P^*(-k)] \tag{6}$$

Use Eqn. 4 for O(k), then drop the quadratic correlation term in $\Phi(k)$ since the speckle spectrum autocorrelation can be assumed to be a delta function, to obtain the relationship between phase and intensity spectra,

$$I(k) = |P(k_l)|^2 \delta(k) + H_{k_l}(k)\Phi(k) \tag{7}$$

linearly relating the intensity spectrum of the image $I(k)$ to the phase spectrum of the rough surface $\Phi(k)$,

$$H_{k_l}(k) = iP(k+k_l)P^*(k_l) - iP^*(-k+k_l)P(k_l) \tag{8}$$

$H_{k_l}(k)$ is the *phase to intensity transfer function* for off-axis illumination with the Koehler source at position k_l in the pupil. It relates the phase spectrum $\Phi(k)$ to intensity spectrum $I(k)$ given that weak phase (Eqn. 2) is valid. Figure 1c shows the transfer function for two such cases - on-axis illumination with defocus as the pupil function, and off-axis illumination with the same defocus. If defocus is centered in the pupil, it shifts with respect to the object spectrum for off-axis illumination (Fig. 1b). Now for broadband speckle, $\Phi(k)$ is uniformly distributed across the spectrum, hence the intensity spectrum ($I(k) = H(k)\Phi(k)$) directly images the phase-to-intensity transfer function $H(k)$ [6] (Fig. 1d).

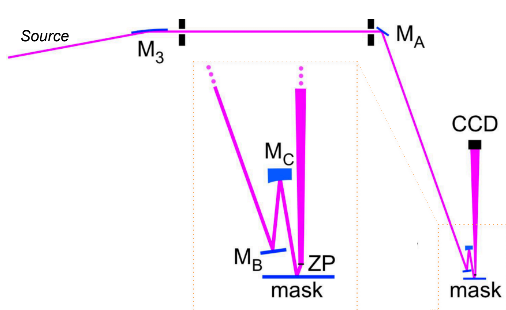

Fig. 2. SHARP is an EUV microscope in reflection geometry, where M's are multilayer reflectors and ZP is a zone plate lens, and mask is a blank object. At EUV wavelength a flat surface even with a few Angstrom roughness creates speckle at the camera, which can be used to characterize the system transfer function.

2. Aberration estimation on the SHARP EUV microscope

SHARP is an EUV microscope at the Lawerence Berkeley National Lab operating in reflection geometry as shown in Fig. 2. A mask blank at the output plane creates natural speckle (Fig. 3a), directly encoding pupil information in the speckle spectra (Fig. 3b). The spectra shows two displaced circles, corresponding to the pupil and its conjugate, with a region of overlap in between (Fig. 3b,c,d). Depending on the aberrations in the system, the transfer function buried in the speckle spectrum has a distinct morphology. In this case it corresponds to $P(k)$ as a shifted defocus that is centered with respect to the object spectrum (Fig. 3e), indicating that the defocus is normal to the incident beam (instead of the central axis), a peculiarity of the reflection geometry of the tool (Fig. 2), where the output beam is always normal to the CCD camera.

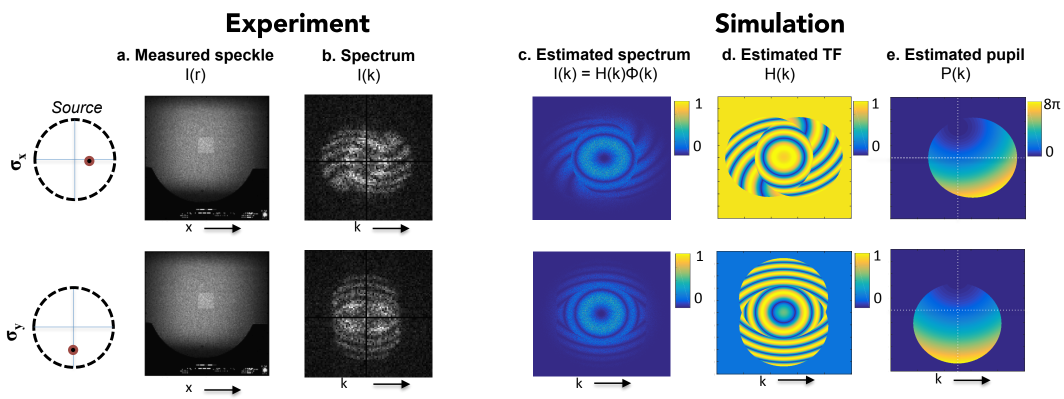

Fig. 3. a,b) Speckle spectrum in an EUV microscope with off-axis illumination (at $k_l/k = 0.3$) shows two overlapping pupils, with a distinct morphology for the source shifted horizontally (top) and vertically (bottom). c,d,e) The structure in the speckle spectrum $I(k)$ reflects the weak phase transfer function $H(k)$, recreated in simulation with a defocus pupil function $P(k)$ centered about the object spectrum while the pupil circle shifts with illumination angle. The recovered pupil can be used for tool calibration, or for object phase recovery from off-axis illumination measurements.

A more rigorous fitting of the aberration shapes to the numerical model will allow estimation of higher order aberrations in the system. The method can be extended to estimate the pupil for the complete 0 to 2π range of azimuthal illumination angles, similar to diffraction tableauxs used in electron microscopy [8, 9], but applicable over larger tilt angles (k_l/k). This will allow characterization of illumination dependent aberrations with the speckle inherent in any image, particularly useful for system alignment, or for methods such as Fourier Ptychography [10] where object reconstruction based on illumination angle diversity needs a good estimate of the pupil at each angle for robust recovery.

3. Acknowledgements

The LBNL EUV program is supported by Eureka, and initial funding for SHARP was from SEMATECH. The Advanced Light Source is supported by the Director, Office of Science, Office of Basic Energy Sciences, of the U.S. Department of Energy under Contract No. DE-AC02-05CH11231. UC Berkeley support by IMPACT+ group of companies - Applied Materials, ARM, ASML, Global Foundries, IBM, Intel, KLA-Tencor, Marvell Technology, Mentor Graphics, Panoramic Tech, Photronics, Qualcomm, San-Disk and Tokyo Electron.

References

1. R. A. Claus, P. P. Naulleau, A. R. Neureuther, and L. Waller, "Quantitative phase retrieval with arbitrary pupil and illumination," Opt. Express **23**, 26,672–26,682 (2015).
2. R. H., "Nonstandard imaging methods in electron microscopy," Ultramicroscopy (1977).
3. M. Born, "Quantenmechanik der Stoßvorgänge," Zeitschrift fur Physik **38**, 803–827 (1926).
4. N. Streibl, "Three-dimensional imaging by a microscope," J. Opt. Soc. Am. A **2**, 121–127 (1985).

5. C. J. R. Sheppard, “Defocused transfer function for a partially coherent microscope and application to phase retrieval,” J. Opt. Soc. Am. A **21**, 828–831 (2004).
6. G. Gunjala, A. Shanker, V. Jaedicke, N. Antipa, and L. Waller, “Optical transfer function characterization using a weak diffuser,” Proceedings of SPIE (2016).
7. D. C. Champeney, *A Handbook of Fourier Theorems, Ch. 11* (Cambridge University Press, 1987). Cambridge Books Online.
8. J. Spence, *Experimental high-resolution electron microscopy*, Monographs on the physics and chemistry of materials (Oxford University Press, 1988).
9. F. Zemlin, K. Weiss, P. Schiske, W. Kunath, and K.-H. Herrmann, “Coma-free alignment of high resolution electron microscopes with the aid of optical diffractograms,” Ultramicroscopy **3**, 49 – 60 (1978).
10. G. Zheng, R. Horstmeyer, and C. Yang, “Wide-field, high-resolution Fourier ptychographic microscopy,” Nature Photonics **7**, 739–745 (2013).